X CONGRESSO NACIONAL DE ENGENHARIA MECÂNICA 2018
20 A 24 DE MAIO DE 2018 SALVADOR – BA – BRASIL

DEVIATION IN FATIGUE LIFE RESULTS DUE TO DIFFERENT METHODS OF OBTAINING CONSTANTS

Caio Ferreira Barros, caiofbarros@gmail.com[1]
Jorge Alberto Rodriguez Durán, jorge.a.r.duran@gmail.com[1]
[1]Universidade Federal Fluminense – Escola de Engenharia Industrial Metalúrgica de Volta Redonda (EEIMVR-UFF), Programa de Pós-graduação em Engenharia Mecânica (PGMEC), Av. dos Trabalhadores, 420, Vila Santa Cecília – Volta Redonda / RJ, 27255-125

Abstract: *Fatigue life can be calculated from local strain amplitudes according to the well known Coffin-Manson relation. For notched bodies, neglecting transient, local strains should follow simultaneously the cyclic stress-strain curve and a stress concentration rule. Occasionally, the fitting constants for the cyclic stress-strain curve are not available and the so called compatible constants are used instead. The present paper evaluates the consequences that this decision have on the final life calculated by the strain approach to fatigue and how divergent results can be generated according to the material and analysis parameters applied. For steels, fatigue life results obtained with the compatible constants consistently represent the results obtained with the experimental constants, without divergence. However, for aluminum, when compared the experimental and compatible methods to obtain the constants, fatigue life results diverge in such a way that, according to the change in the values of the analysis parameters, such as stress amplitude, stress ratio and stress concentration factor, the results obtained using the constants from the compatible method can be either equivalent or slightly non-conservative, or even considerably conservative in relation to the results obtained with the constants from the experimental method.*
Keywords: *strain-based fatigue, aluminum fatigue, cyclic stress-strain constants, strain-life constants*

1. INTRODUCTION

Through the strain-based approach to fatigue, life can be obtained using the cyclic stress-strain curve in relation to a stress concentration rule, as Neuber's rule, to determine the associated strain amplitude. Then, through the Coffin-Manson equation, obtain the life directly associated with that strain amplitude. To describe the cyclic stress-strain curve is used the Ramberg-Osgood equation, Eq. (1):

$$\varepsilon_a = \frac{\sigma_a}{E} + \left(\frac{\sigma_a}{H'}\right)^{1/n'} \tag{1}$$

Where σ_a and ε_a are the stress and strain amplitudes, respectively, E is modulus of elasticity, H' is the cyclic strength coefficient, and n' is the cyclic strain hardening exponent. And to describe the strain-life relation is used the Coffin-Manson equation, Eq. (2):

$$\varepsilon_a = \frac{\sigma'_f}{E}\left(2N_f\right)^b + \varepsilon'_f\left(2N_f\right)^c \tag{2}$$

Where N_f is the number of cycles to failure, σ'_f is the fatigue strength coefficient, b is the fatigue strength exponent, ε'_f is the fatigue ductility coefficient and c is the fatigue ductility exponent. Between the six constants: H', n', σ'_f, b, ε'_f and c, only four are independent. Meaning that two can be calculated from the other four through Eq. (3) and Eq. (4).

$$H' = \frac{\sigma'_f}{\left(\varepsilon'_f\right)^{b/c}} \tag{3}$$

$$n' = \frac{b}{c} \tag{4}$$

To calculate the stress-strain curve through the Ramberg-Osgood equation, Eq. (1), and the strain-life curve through the Coffin-Manson equation, Eq. (2), these six material constants are necessary. They can be obtained either by fitting the experimental data or by the mathematical approach from the other properties, producing the compatible constants. But, as most of the time the experimental data is not readily available, fatigue life is calculated using the compatible values. For some cases, this approach can result in adequate life results, equivalent to those that would be obtained with the experimental constants, and, for other cases, some deviation can be found between life results obtained with the

compatible constants and the experimental constants. In recent years, studies have been conducted in order to verify the reliability and improve the different methods available to estimate material constants, such as in Marohnić *et al.* (2015); Meggiolaro and Castro (2004). As shown in Meggiolaro and Castro (2004), for steels, the life results for provided by both methods are usually quite equivalent. However, for aluminum, there is a deviation that should be considered when drawing up conclusions about the analysis.

In this paper the effects caused in fatigue lives, because of the method used to obtain the constants, will be demonstrated and compared, observing especially which combinations of analysis parameters were used. Thus showing, in what situations it is reasonable and reliable to use the calculated constants, and in which situations which method is more conservative.

2. COMPUTATIONAL PROCEDURE

2.1 Analysis Parameters and Materials Properties

Regarding the analysis parameters, multiple combinations between the values of nominal stress amplitude, S_a, and nominal maximum stress, S_{max}, were used in order to represent loads with stress ratio, R, within the following limits: $-1 \leq R \leq 0.5$. With nominal stress amplitude limited to 30 % of ultimate tensile strength, σ_u, and with nominal maximum stress limited to 70 % of ultimate tensile strength. To demonstrate the influence of the notch on the calculated fatigue lives, usual values were selected for the elastic stress concentration factor, k_t, as in Dowling (2012). The analysis was performed individually on each material for each value of k_t and combinations of S_a and S_{max}.

The materials and their properties used for the analysis are presented in Tab. 1. Where σ_u is ultimate tensile strength, E is modulus of elasticity, H' is cyclic strength coefficient, n' is cyclic strain hardening exponent, σ'_f is fatigue strength coefficient, b is fatigue strength exponent, ε'_f is fatigue ductility coefficient and c is fatigue ductility exponent. These properties were sourced from Dowling (2012); SAE Standard J1099 (1998); Wong (1984); Lease and Stephens (1991); Boller and Seeger (1987); Burk and Lawrence (1978); Chen and Lawrence (1979).

Table 1: **Materials properties.**

Material	σ_u (MPa)	E (MPa)	H' (MPa)	n'	σ'_f (MPa)	b	ε'_f	c
1100	110	69000	154	0.144	166	-0.096	1.643	-0.669
2014-T6 (Hand Forged)	483	72700	605	0.049	976	-0.12	0.88	-0.88
2014-T6	510	69000	963	0.132	1008	-0.114	1.418	-0.87
2024-T3	490	70280	843	0.109	835	-0.096	0.174	-0.644
2024-T351	469	73100	662	0.07	927	-0.113	0.409	-0.713
2024-T4 (Prestrained)	476	73100	738	0.08	1294	-0.142	0.327	-0.645
2024-T4	476	70430	808	0.098	764	-0.075	0.334	-0.649
5083-0 (93 HB)	294	71000	580	0.114	711	-0.122	0.405	-0.692
5083-H12	385	69000	417	0.035	650	-0.094	2.26	-1.01
5183-0 (Weld Metal - 92 HB)	299	71000	507	0.072	638	-0.107	0.581	-0.89
5454 (Forged)	334	69000	373	0.047	554	-0.089	0.31	-0.62
5456-H311	400	69000	817	0.145	826	-0.115	1.076	-0.797
6061-T6 (Forged)	389	69000	422	0.03	689	-0.094	0.35	-0.67
6061-T6 (Hand Forged)	340	72700	416	0.042	645	-0.097	0.22	-0.6
6061-T6 (Sheet)	314	69600	426	0.062	535	-0.082	1.34	-0.83
7075-T6	578	71000	977	0.106	1466	-0.143	0.262	-0.619
7075-T6	572	72230	521	0.045	776	-0.0951	2.56	-0.987
7075-T6	579	71000	2514	0.146	1917	-0.176	0.156	-0.526
7075-T651	580	70000	852	0.074	1231	-0.122	0.263	-0.806
7175-T73 (Hand Forged)	524	71300	529	0.033	765	-0.082	6.18	-1.14
A356-T6 (Cast)	252	71000	394	0.0615	495	-0.117	0.0177	-0.458
A356-T6 (Cast)	266	70000	383	0.0499	502	-0.119	0.0166	-0.544
A356-T6 (Cast)	283	70000	379	0.0429	594	-0.124	0.0269	-0.53
AISI 4340 (Aircraft Qual.)	1172	207000	1655	0.131	1758	-0.0977	2.12	-0.774
AISI 4340 (409 HB)	1468	200000	1910	0.123	1879	-0.0859	0.64	-0.636
Man-Ten (Hot Rolled)	557	203000	1096	0.187	1089	-0.115	0.912	-0.606
RQC-100 (Roller Q & T)	758	200000	903	0.0905	938	-0.0648	1.38	-0.704
SAE 1015 (Normalized)	415	207000	1349	0.282	1020	-0.138	0.439	-0.513
SAE 1045 (HR & Norm.)	621	202000	1258	0.208	948	-0.092	0.26	-0.445
SAE 4142 (Q & T - 380 HB)	1413	207000	2210	0.133	2140	-0.0944	0.637	-0.761
SAE 4142 (Q & T - 450 HB)	1757	207000	2080	0.093	1937	-0.0762	0.706	-0.869
SAE 4142 (Q & T - 560 HB)	2240	207000	4140	0.126	3410	-0.121	0.0732	-0.805

2.2 Life Calculation Procedure

With the Ramberg-Osgood equation, Eq. (1), two cyclic stress-strain curves were generated. For one curve, the constants H' and n' used were extracted from the curves fitted to the experimental data. And for the other curve, those same constants were calculated through Eq. (3) and Eq. (4), respectively.

As a stress concentration rule, Neuber's rule was used as established in Eq. (5). With this equation, two other curves were generated in order to apply the effect of the stress concentration factor, k_t, to the analysis. The single factor that differentiates both these generated curves is the nominal stress value, S. For one curve, it is used the nominal stress amplitude, S_a, and for the other, the nominal maximum stress, S_{max}.

$$\sigma_a \varepsilon_a = \frac{(k_t S)^2}{E} \tag{5}$$

Plotting both curves obtained through Eq. (1) and both obtained through Eq. (5) in the same graph, as exemplified in Fig. 1, four points of intersection were obtained. There are two points of intersection on each Ramberg-Osgood curve, where the coordinates of each point are determined by the Neuber curve used for the intersection. For the Neuber curve based on S_a, the coordinates are σ_a and ε_a, and for the other one, which is based on S_{max}, the coordinates are σ_{max} and ε_{max}. Therefore, for each method (compatible and experimental) there is a set of values for strain amplitude, ε_a, maximum strain, ε_{max}, stress amplitude, σ_a, and maximum stress, σ_{max}.

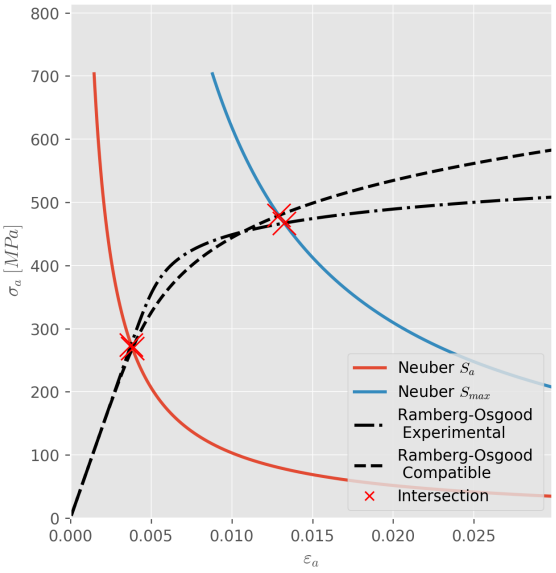

Figure 1: **Demonstration of the intersection between the curves generated with Ramberg-Osgood and with Neuber's Rule.**

The relation between the values of strain amplitude, ε_a, and life, N_f, is represented by the Coffin-Manson equation, Eq. (2). However, since cyclic loads with mean stress, σ_m, different than zero were used for the analysis, the effect of the mean stress must be included in the equation. For this purpose, the Modified Morrow Approach, Eq. (6), was used. Where, for each method of obtaining the constants, σ_m was calculated according to its values of σ_a and σ_{max} using Eq. (7).

$$\varepsilon_a = \frac{\sigma'_f}{E}\left(1 - \frac{\sigma_m}{\sigma'_f}\right)(2N_f)^b + \varepsilon'_f (2N_f)^c \tag{6}$$

$$\sigma_m = \sigma_{max} - \sigma_a \tag{7}$$

To find the life value associated with each stress amplitude through the Modified Morrow Approach, a intersection method was applied. For this purpose, in the same strain-life graph, were plotted the curves generated with Eq. (6) for each method of obtaining the constants and a horizontal line representing the value of ε_a for the corresponding method, as obtained in the previous graph, shown in Fig. 2. In this graph, one point of intersection was found between the curves of each method, so in total two points were found. The coordinates of each point indicate the life, N_f, associated with each strain amplitude, ε_a.

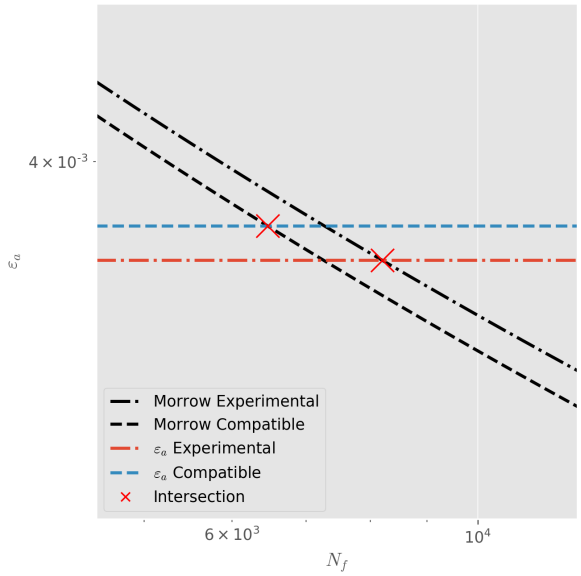

Figure 2: **Demonstration of the intersection between the generated Morrow curve and the strain amplitude (ε_a) value.**

3. RESULTS AND DISCUSSION

In possession of life values obtained with the constants from the experimental and compatible methods, a comparison was made between both values. On a life-life graph (N_f vs N_f) with the same ratio between both axes that are on a logarithmic scale, every point was plotted using as coordinates the life values obtained with the constants from each method. Were plotted as well reference lines, one representing where the lives are equivalent, and the others are scatter bands of factor 1.25, 1.5 and 2, where lives for one method are multiple times what resulted for the other method, as shown in Troshchenko and Khamaza (2010).

Initially, the results for all steels, when using all possible combination of parameters for the analysis, are shown in Fig. 3, in order to demonstrate that both methods used to obtain the constants generate equivalent results for this type of material. The lives calculated by both methods are mostly equivalent, regardless of the value assumed by each of the analysis parameters (k_t, S_a and S_{max}), with only a few analysis generating results outside the scatter band of 1.25.

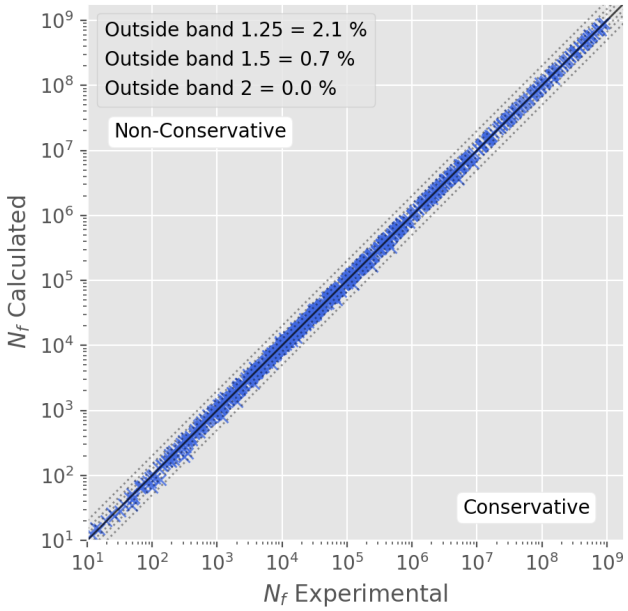

Figure 3: **General life results for all steels.**

The results for all aluminum are shown in Fig. 4, where all possible combination of parameters for the analysis are used, similarly to Fig. 3. It is promptly observed that there is a greater dispersion in results compared to the steel results,

especially in the low life region, where the results obtained through the compatible constants are more conservative. Considering all the available data, 21.1 % of all results are outside the 1.25 scatter band, and focusing only in the low life region, an even greater proportion of the results are outside the considered scatter bands.

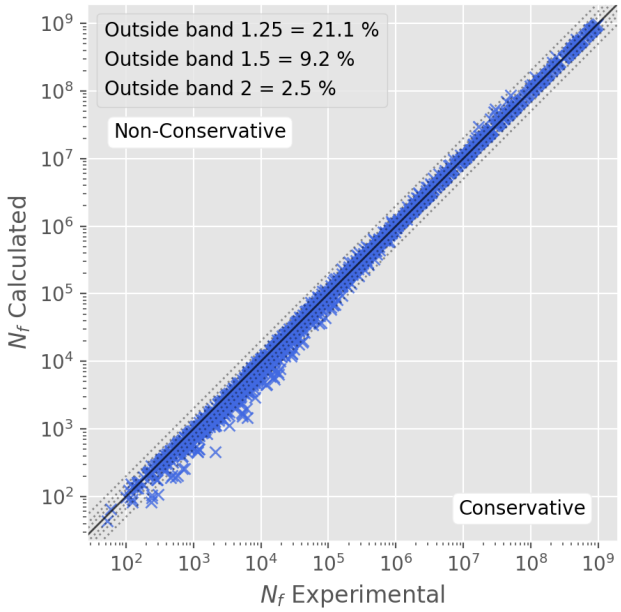

Figure 4: **General life results for all aluminum.**

Continuing with a more in depth analysis of the aluminum, are presented in Figs. 5, 6, 7 and 8 detailed results for all materials of this type, separated by stress ratio, R, where it is possible to observe the effects caused by the change in each of the analysis parameters. Each figure shows on its vertical axis the ratio between the lives obtained with the calculated constants, $N_{f\,calc}$, and the experimental constants, $N_{f\,exp}$, represented in logarithmic scale, where values below 1.0 represent conservative results and values above this threshold represent non-conservative results. On its horizontal axis, is the ratio between stress amplitude, S_a, and ultimate tensile strength, σ_u, which is used in order to keep all materials in a comparable basis for the values of stress amplitude.

In Tabs. 2, 3, 4 and 5 are shown the statistical analysis for each one of the Figs. 5, 6, 7 and 8, respectively. For each combination of R, k_t and S_a/σ_u is presented a set of statistical evaluations condensing results from all materials. Each set contains: geometric mean and geometric standard deviation.

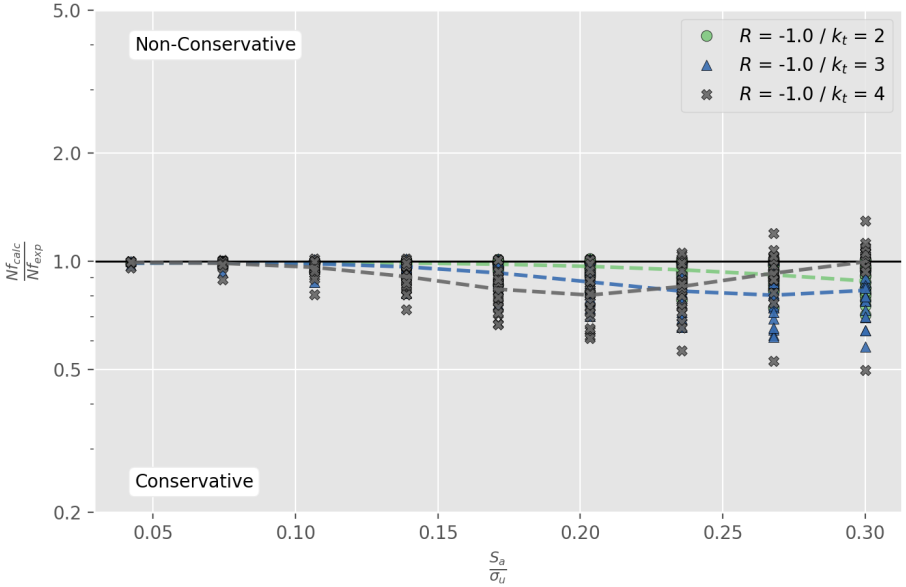

Figure 5: **Change in life ratio with stress amplitude and stress concentration factor for R = - 1.0.**

Table 2: **Statistical analysis for R = - 1.0.**

S_a/σ_u	$R=-1.0 \mid K_t=2.0$		$R=-1.0 \mid K_t=3.0$		$R=-1.0 \mid K_t=4.0$	
	Geometric Mean	Geometric Standard Deviation	Geometric Mean	Geometric Standard Deviation	Geometric Mean	Geometric Standard Deviation
0.04	0.989	0	0.987	1.016	0.992	1.014
0.07	0.992	1.014	0.992	1.018	0.987	1.027
0.11	0.992	1.017	0.984	1.031	0.962	1.052
0.14	0.989	1.024	0.965	1.05	0.906	1.09
0.17	0.981	1.034	0.928	1.075	0.836	1.132
0.2	0.968	1.047	0.876	1.108	0.805	1.173
0.24	0.947	1.063	0.826	1.139	0.851	1.178
0.27	0.917	1.083	0.804	1.17	0.926	1.167
0.3	0.881	1.105	0.83	1.181	0.996	1.183

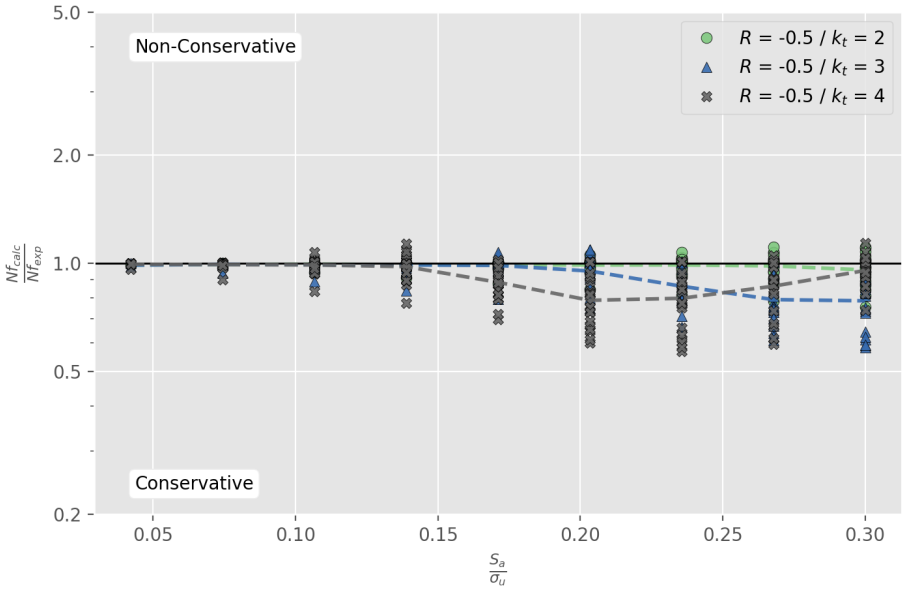

Figure 6: **Change in life ratio with stress amplitude and stress concentration factor for R = - 0.5.**

Table 3: **Statistical analysis for R = - 0.5.**

S_a/σ_u	$R=-0.5 \mid K_t=2.0$		$R=-0.5 \mid K_t=3.0$		$R=-0.5 \mid K_t=4.0$	
	Geometric Mean	Geometric Standard Deviation	Geometric Mean	Geometric Standard Deviation	Geometric Mean	Geometric Standard Deviation
0.04	0.989	0	0.988	1.015	0.994	1.013
0.07	0.992	1.013	0.994	1.016	0.991	1.023
0.11	0.994	1.015	0.991	1.026	0.989	1.048
0.14	0.992	1.021	0.989	1.046	0.979	1.087
0.17	0.99	1.03	0.986	1.069	0.885	1.109
0.2	0.989	1.043	0.951	1.104	0.789	1.172
0.24	0.989	1.058	0.863	1.116	0.799	1.206
0.27	0.983	1.078	0.792	1.166	0.863	1.18
0.3	0.958	1.103	0.786	1.202	0.955	1.099

Starting the analysis with $R = -1$ at Fig. 5, for all values of k_t, the mean values of life ratio are conservative throughout the whole range of S_a/σ_u values, especially for the second half, where $0.15 < S_a/\sigma_u < 0.30$. The behavior exhibited in Fig. 6, for $R = -0.5$, shows similar results for mean values and standard deviation as seen at Fig. 5.

In Fig. 7 with $R = 0$, there is a shift in the mean values of life ratio to the non-conservative side, even though for the higher values of S_a/σ_u the means are still conservative. The range of S_a/σ_u for which this occurs depends on the value of k_t, for higher values the shift occurs at a lower range of S_a/σ_u.

And in Fig. 8 with $R = 0.5$, the mean value for life ratio shifts further away from the equivalent line throughout the whole available range of S_a/σ_u and, at the same time, the peak values occurs at lower values of S_a/σ_u than at $R = 0$. Meaning more conservative results for higher values of S_a/σ_u, and more non-conservative results for lower values of S_a/σ_u.

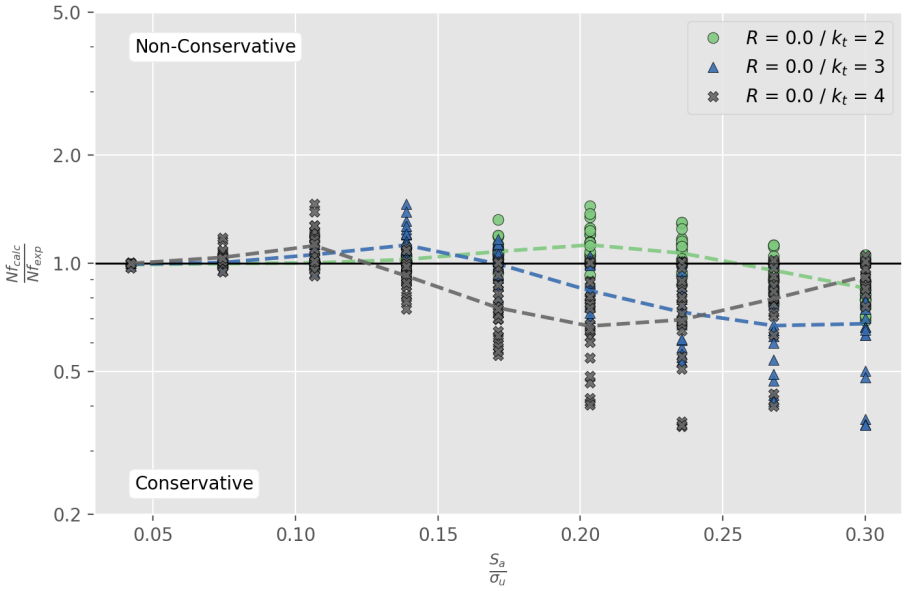

Figure 7: **Change in life ratio with stress amplitude and stress concentration factor for R = 0.0.**

Table 4: **Statistical analysis for R = 0.0.**

S_a/σ_u	$R = 0.0 \mid K_t = 2.0$		$R = 0.0 \mid K_t = 3.0$		$R = 0.0 \mid K_t = 4.0$	
	Geometric Mean	Geometric Standard Deviation	Geometric Mean	Geometric Standard Deviation	Geometric Mean	Geometric Standard Deviation
0.04	0.991	0	0.994	1.01	0.999	1.008
0.07	0.998	1.008	1.005	1.013	1.038	1.048
0.11	1.002	1.011	1.057	1.063	1.119	1.128
0.14	1.024	1.033	1.124	1.128	0.922	1.109
0.17	1.078	1.077	0.995	1.103	0.751	1.211
0.2	1.125	1.125	0.839	1.143	0.669	1.34
0.24	1.067	1.115	0.731	1.234	0.696	1.389
0.27	0.956	1.104	0.67	1.331	0.797	1.284
0.3	0.853	1.136	0.679	1.387	0.921	1.09

Looking at Figs. 5, 6, 7 and 8, the behavior of the data in relation to the increase of R becomes clearer. Its increase causes the profile of the mean curves to move to lower values of S_a/σ_u and, at the same time, it causes distress on conservativity of the results, meaning that, with higher R values, the mean values move away from the equivalent line.

The dispersion of life ratio values, demonstrated by the standard deviation shown in Tabs. 2, 3, 4 and 5, is increased by the increase in R, k_t and S_a/σ_u.

As the value of S_a is increased, the deviation found between the methods is also increased, demonstrated by the fact that the for higher values of S_a, the mean value is further away from the equivalent line than for lower values. Thus, there is a greater sensitivity to alteration in the other parameters at higher values of S_a.

Analyzing the general influence of k_t, it is noticed that the life ratio results are modified by the increase in k_t, in such a way that similar results occur at lower values of S_a/σ_u for higher k_t values. Maintaining similar behavior to that presented in smaller values of k_t, but occurring at lower values of S_a/σ_u.

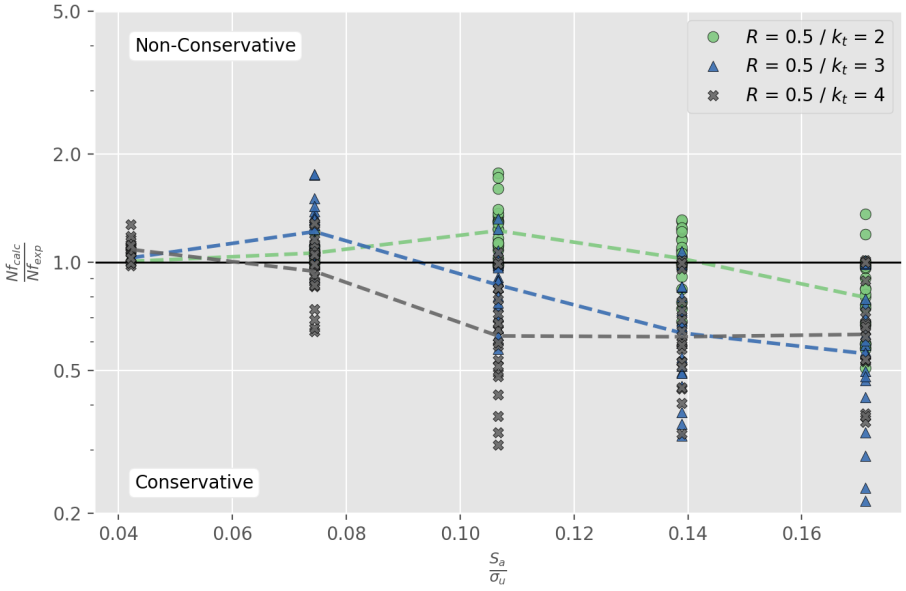

Figure 8: **Change in life ratio with stress amplitude and stress concentration factor for R = 0.5.**

Table 5: **Statistical analysis for R = 0.5.**

	$R = 0.5 \mid K_t = 2.0$		$R = 0.5 \mid K_t = 3.0$		$R = 0.5 \mid K_t = 4.0$	
S_a/σ_u	Geometric Mean	Geometric Standard Deviation	Geometric Mean	Geometric Standard Deviation	Geometric Mean	Geometric Standard Deviation
0.04	1.006	0	1.029	1.009	1.085	1.067
0.07	1.061	1.052	1.217	1.194	0.944	1.21
0.11	1.225	1.188	0.865	1.249	0.624	1.429
0.14	1.024	1.19	0.636	1.412	0.62	1.378
0.17	0.799	1.297	0.557	1.559	0.63	1.405

4. CONCLUSIONS

From the study carried out in this paper, using well established equations for the solutions, it was discussed how the cyclic stress-strain and strain-life constants obtained by both methods produce consistent results for steels, but for aluminum the results should be examined more carefully according to the parameters of the study.

Special attention should be given for analyses with short lives, given the level of dispersion outside the control bands shown in Fig. 4. High level of divergence between life results can be found as well for a combination of $R > 0$ and $K_t > 2$. For these situations, the results generated by the calculated constants are conservative, with the mean value close to 65 % of $N_{f\,exp}$ for the higher values of S_a/σ_u, but non-conservative for lower values of S_a/σ_u.

It is also worth noting that for aluminum, there are some situations with mean life ratio close to 1, where they are equivalent: for values of $R < 0$ and $k_t = 2$, where the lives are equivalent for most values of S_a/σ_u; and in general for low values of k_t, where the deviations tend to be less amplified, which is true even for some combinations of R and S_a/σ_u that would result in larger differences in higher values of k_t.

5. REFERENCES

Boller, C. and Seeger, T., 1987. *Materials data for cyclic loading*, Vol. 42. Elsevier, Amsterdam.

Burk, J.D. and Lawrence, F.V., 1978. "The effect of residual stresses on weld fatigue life". Technical report, University of Illinois.

Chen, W.C. and Lawrence, F.V., 1979. "A model for joining the fatigue crack initiation and propagation analyses". Technical report, University of Illinois.

Dowling, N.E., 2012. *Mechanical Behavior of Materials: Engineering Methods for Deformation, Fracture, and Fatigue; 4th ed.* Pearson, Boston, MA.

Lease, K. and Stephens, R., 1991. "Verification of variable amplitude fatigue life methodologies for a cast aluminum alloy". Technical report, SAE Technical Paper.

Marohnić, T., Basan, R. and Franulović, M., 2015. "Evaluation of the possibility of estimating cyclic stress-strain param-

eters and curves from monotonic properties of steels". *Procedia Engineering*, Vol. 101, No. Supplement C, pp. 277 – 284.

Meggiolaro, M. and Castro, J., 2004. "Statistical evaluation of strain-life fatigue crack initiation predictions". *International Journal of Fatigue*, Vol. 26, No. 5, pp. 463 – 476.

SAE Standard J1099, 1998. "Technical Report on Low Cycle Fatigue Properties Ferrous and Non-Ferrous of Materials". Technical report, SAE International.

Troshchenko, V. and Khamaza, L., 2010. "Strain–life curves of steels and methods for determining the curve parameters. part 1. conventional methods". *Strength of materials*, Vol. 42, No. 6, pp. 647–659.

Wong, W.A., 1984. "Monotonic and cyclic fatigue properties of automotive aluminum alloys". Technical report, SAE Technical Paper.

6. RESPONSIBILITY NOTICE

The authors are the only responsible for the printed material included in this paper.